

SLC7A8 overexpression inhibits the growth and metastasis of lung adenocarcinoma and is correlated with a dismal prognosis

Fang-Ming Wang^{1,*}, Li-Qiang Xu^{2,*}, Zhong-Chao Zhang^{3,*}, Qiang Guo^{2,*}, Zhi-Peng Du³, Yue Lei⁴, Xu Han³, Chuang-Yan Wu¹, Feng Zhao¹, Jiu-Ling Chen¹

¹Department of Thoracic Surgery, Union Hospital, Tongji Medical College, Huazhong University of Science and Technology, Wuhan, China

²Department of Cardiothoracic Surgery, Taihe Hospital, Hubei University of Medicine, Shiyan, China

³Department of Gastroenterology, Institute of Liver and Gastrointestinal Diseases, Tongji Hospital, Tongji Medical College, Huazhong University of Science and Technology, Wuhan, China

⁴Department of Blood Transfusion, Taihe Hospital, Hubei University of Medicine, Shiyan, China

*Equal contribution and share first authorship

Correspondence to: Jiu-Ling Chen, Feng Zhao; **email:** jiulingchen@hust.edu.cn; tonyzf_89@163.com, <https://orcid.org/0009-0001-4326-3455>

Keywords: *SLC7A8*, lung adenocarcinoma, prognosis, TCGA, immune infiltration

Received: July 6, 2023

Accepted: December 1, 2023

Published: January 18, 2024

Copyright: © 2024 Wang et al. This is an open access article distributed under the terms of the [Creative Commons Attribution License](https://creativecommons.org/licenses/by/4.0/) (CC BY 4.0), which permits unrestricted use, distribution, and reproduction in any medium, provided the original author and source are credited.

ABSTRACT

Background: Overexpression of solute carrier family 7 member 8 (*SLC7A8*) has been shown to relate to the survival time and tumor progression in cancer patients. However, the role of *SLC7A8* in lung adenocarcinoma (LUAD) is still obscure.

Method: The relationships between *SLC7A8* expression in LUAD tissues and clinical values as well as immune infiltration were explored through bioinformatics. The functions and pathways of *SLC7A8* in LUAD were investigated using Kyoto Encyclopedia of Genes and Genomes enrichment analysis, Gene Set Enrichment Analysis, Western blotting, and other methods.

Results: We found that the expression of *SLC7A8* was decreased significantly in LUAD tissues compared with normal tissues, which was related to the dismal survival time and disease progression. Moreover, it carried diagnostic value in LUAD and was a risk factor for dismal prognosis. Receiver operating characteristic curve analysis indicated that the expression level of *SLC7A8* carried significant diagnostic value in LUAD. Overexpression of *SLC7A8* inhibited the proliferation, invasion, and migration of LUAD cells, likely through a mechanism involving the cell cycle. *SLC7A8* expression in LUAD was significantly correlated with the infiltration of immune cells, especially B cells, interstitial dendritic cells, mast cells, CD56 bright cells, natural killer cells, plasmacytoid dendritic cells, T follicular helper cells, T helper 2 and 17 cells, and immune factors.

Conclusion: The downregulation of *SLC7A8* was related to a dismal prognosis and immune cell infiltration in LUAD. Increasing the expression of *SLC7A8* inhibited the growth and migration of LUAD cells, thereby improving the prognosis of patients.

INTRODUCTION

Lung cancer has become one of the leading causes of mortality in the world [1]. Of its different pathological subtypes, non-small cell lung cancer (NSCLC) accounts

for about 85% of all lung cancer cases, and lung adenocarcinoma (LUAD) constitutes the highest proportion of NSCLC cases [2]. The relationship between the expression of certain genes and LUAD progression has been increasingly investigated [3–5]. For example, the

decreased expression of *TNFAIP3*, an anti-inflammatory gene that helps maintain the inflammatory balance, reduced the proportion of CD8⁺ T cells, thus assisting LUAD cells in immune evasion. Moreover, it caused anti-programmed cell death protein 1 monotherapy to be ineffective and led to poor prognosis in LUAD patients [5].

The expression level of *SLC7A8*, which encodes large neutral amino acid transporter small subunit 2, was shown to be related to tumor progression [6–9]. *SLC7A8* was highly expressed in estrogen receptor (ER)-positive breast cancer and was a marker of good prognosis in these patients [6]. In uterine leiomyoma tissues, luteinizing hormone upregulated *SLC7A8*. Knockdown of *SLC7A8* enhanced the proliferation of uterine leiomyoma cells [7]. A mutation in *SLC7A8* reduced the efficacy of the combination of cisplatin and verapamil for treating esophageal squamous carcinoma and induced the development of drug resistance [8]. Asada et al. showed that *SLC7A8* overexpression improved the survival rate of LUAD patients [9]. However, the role of *SLC7A8* in LUAD progression is still obscure.

This study aimed to further elucidate the relationship between *SLC7A8* expression and LUAD prognostic factors using bioinformatics and cell models. We also examined the role of *SLC7A8* in LUAD cell growth and metastasis *in vitro*.

RESULTS

The expression of *SLC7A8* was attenuated in LUAD

The transcripts per million (TPM) data retrieved from The Cancer Genome Atlas (TCGA) and Xena showed that *SLC7A8* was downregulated in LUAD tissues compared with normal lung tissues (Figure 1).

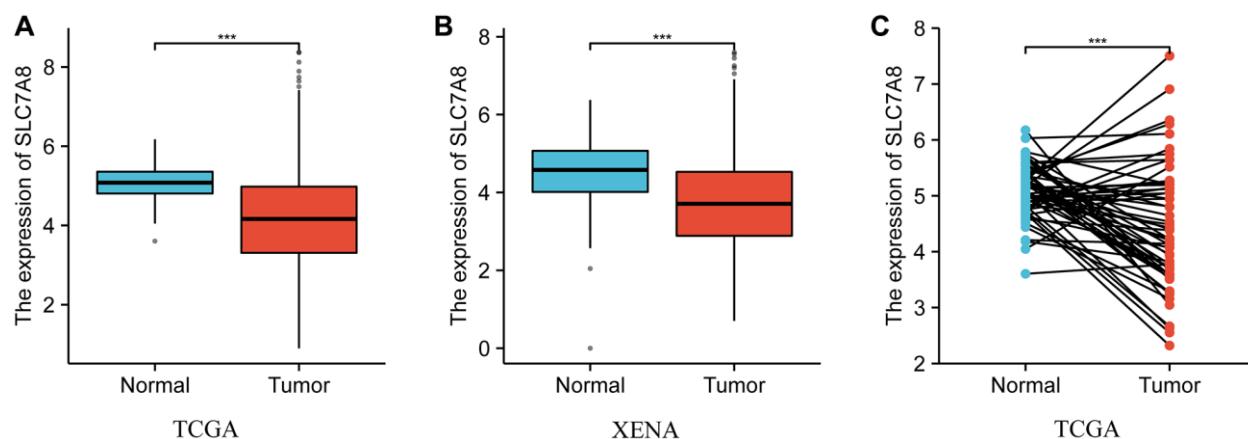


Figure 1. The expression level of *SLC7A8* in LUAD based on TPM data from TCGA and Xena. (A) TPM data of unpaired tissues from TCGA. (B) TPM data of unpaired tissues from Xena. (C) TPM data of paired tissues from TCGA. Abbreviations: LUAD: lung adenocarcinoma; TCGA: The Cancer Genome Atlas; TPM: transcripts per million.

The expression of *SLC7A8* was lower in unpaired LUAD tissues than in normal tissues from TCGA and Xena (Figure 1A, 1B) and in paired LUAD tissues from TCGA (Figure 1C).

Diagnostic value of *SLC7A8* in LUAD

Receiver operating characteristic (ROC) curve analysis indicated that the expression level of *SLC7A8* carried significant diagnostic value in LUAD. The area under the curve values of ROC curves plotted based on *SLC7A8* expression data from TCGA and Xena were 0.750 and 0.707, respectively (Figure 2A, 2B), highlighting the important diagnostic value of *SLC7A8* in LUAD.

Low expression of *SLC7A8* was associated with poor prognosis in LUAD patients

Prognostic data based on the TPM values from TCGA revealed that low expression of *SLC7A8* was associated with poor prognosis in LUAD patients, especially with shorter overall survival (OS), disease-specific survival (DSS), and progression-free interval (PFI) (Figure 3A–3C). Cox regression analysis (Table 1) confirmed the association between low *SLC7A8* expression and poor patient prognosis. A nomogram constructed based on the primary therapy outcome, T stage, N stage, M stage, and *SLC7A8* expression accurately predicted patient prognosis (Figure 4).

SLC7A8 overexpression inhibited the proliferation, migration, and invasion of LUAD cells

The expression of *SLC7A8* was significantly higher in BEAS-2B cells than in A549 and H1299 cells (Figure 5A). Gene Ontology analysis showed that 679 genes co-expressed with *SLC7A8* were correlated with cell cycle progression (Table 2). The overexpression of

SLC7A8 in A549 and H1299 cells was successfully verified using Western blotting (Figure 5B). The Transwell assay showed that the number of A549 and H1299 cells in the *SLC7A8*-overexpression group were significantly lower than in the control group (Figure 5C). Overexpressing *SLC7A8* inhibited the migration of A549 and H1299 cells, as evidenced by the wound healing assay (Figure 5D). The Cell Counting Kit-8 (CCK-8) assay also demonstrated that the number of A549 and H1299 cells significantly decreased in the *SLC7A8*-overexpression group compared with the control group (Figure 6A). The colony forming assay showed that the ability of cells to proliferate was lower

in the *SLC7A8*-overexpression group (Figure 6B). These findings indicate that overexpressing *SLC7A8* inhibited the proliferation, migration, and invasion of LUAD cells.

Mechanisms and protein-protein interaction (PPI) network of SLC7A8

The PPI network shows protein relationships among *SLC7A8*-related genes (Figure 7). Kyoto Encyclopedia of Genes and Genomes enrichment analysis and Gene Set Enrichment Analysis (GSEA) indicated that *SLC7A8* influenced the cell cycle and DNA replication (Figure 8A–8F and Table 2). We conducted relevant

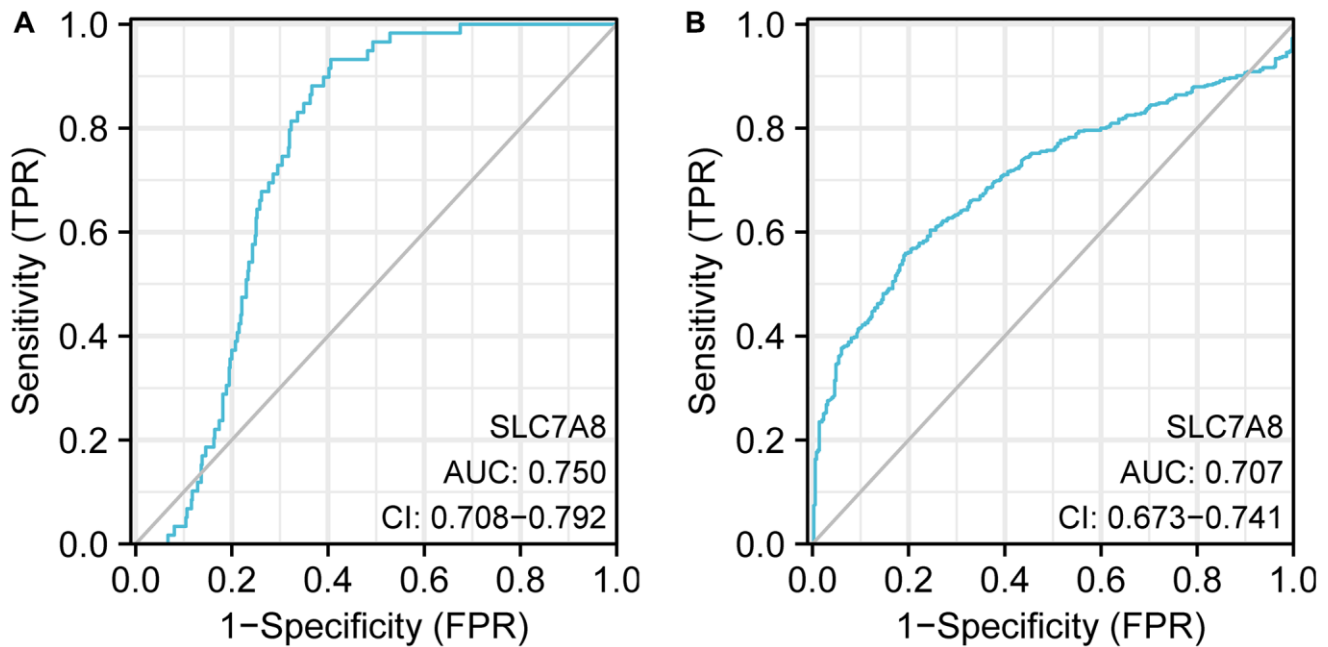


Figure 2. ROC curve analysis indicating the diagnostic value of *SLC7A8* in LUAD. (A) TPM data from TCGA. (B) TPM data from Xena. Abbreviation: ROC: receiver operating characteristic.

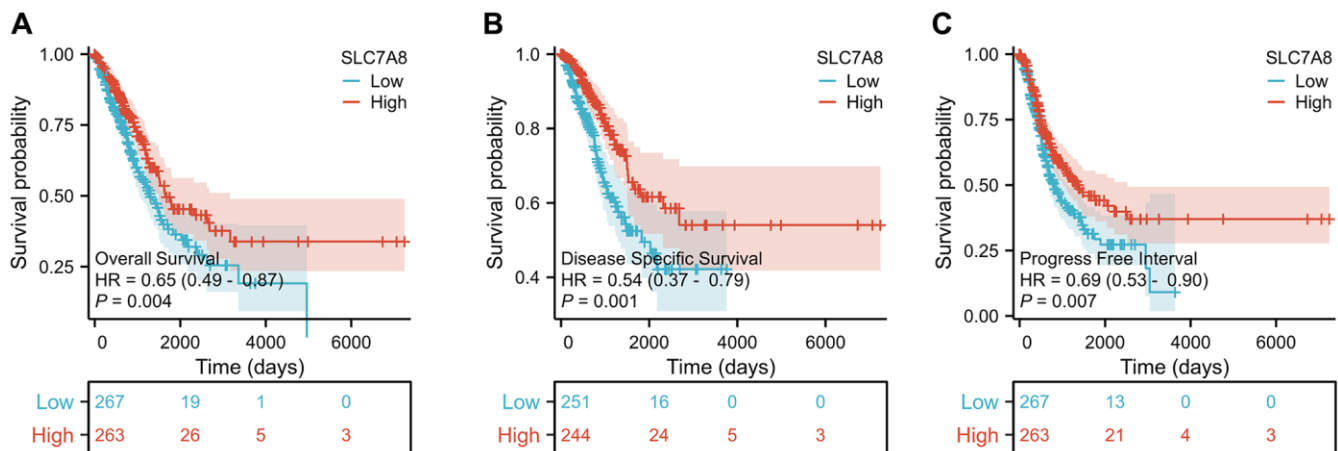


Figure 3. Expression level of *SLC7A8* is associated with the prognosis of LUAD patients. *SLC7A8* expression is associated with (A) OS in LUAD patients, (B) DSS in LUAD patients, (C) PFI in LUAD patients. Abbreviations: OS: overall survival; DSS: disease-specific survival; PFI: progression-free interval.

Table 1. Cox regression analysis reveals the prognostic factors in LUAD.

Characteristics	N	HR (95% CI)	P-value
T stage	527		<0.001
T1	176	Reference	
T2	285	1.507 (1.059–2.146)	0.023
T3 and T4	66	3.095 (1.967–4.868)	<0.001
N stage	514		<0.001
N0	345	Reference	
N1	96	2.293 (1.632–3.221)	<0.001
N2 and N3	73	2.993 (2.057–4.354)	<0.001
M stage	381		0.010
M0	356	Reference	
M1	25	2.176 (1.272–3.722)	0.005
Primary therapy outcome	442		<0.001
PD	71	Reference	
SD	38	0.289 (0.141–0.592)	<0.001
PR	5	0.702 (0.170–2.897)	0.625
CR	328	0.266 (0.185–0.382)	<0.001
Race	472		0.191
Asian	8	Reference	
Black or African American	55	1.911 (0.254–14.382)	0.529
White	409	2.714 (0.380–19.403)	0.320
Gender	530		0.570
Female	283	Reference	
Male	247	1.087 (0.816–1.448)	0.569
Age	520		0.185
≤65	257	Reference	
>65	263	1.216 (0.910–1.625)	0.186
SLC7A8	530		0.004
Low	267	Reference	
High	263	0.655 (0.491–0.874)	0.004

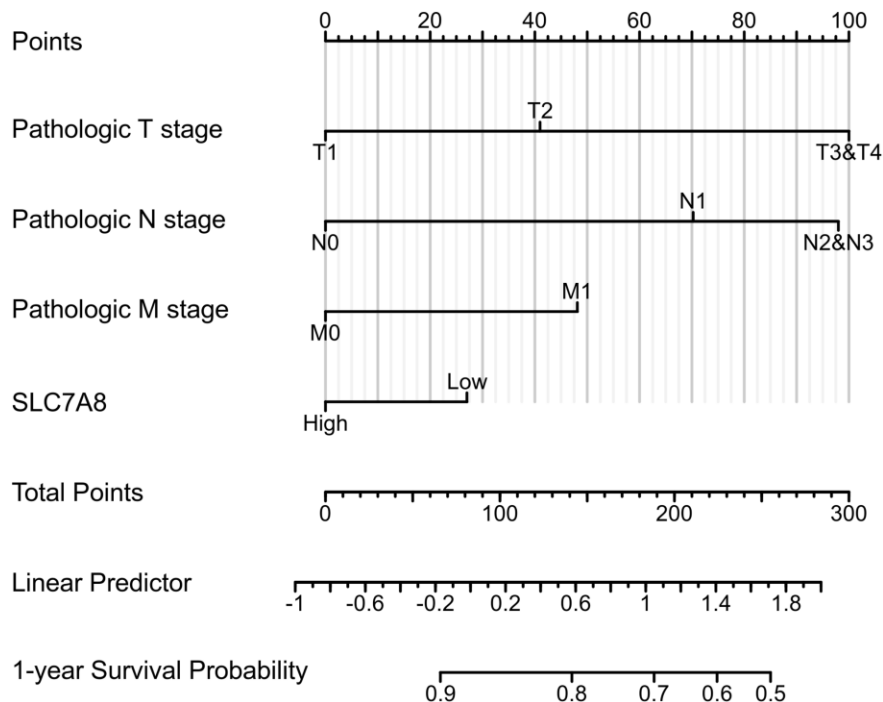


Figure 4. The nomogram shows the correlation between low expression of *SLC7A8* and poor prognosis of LUAD.

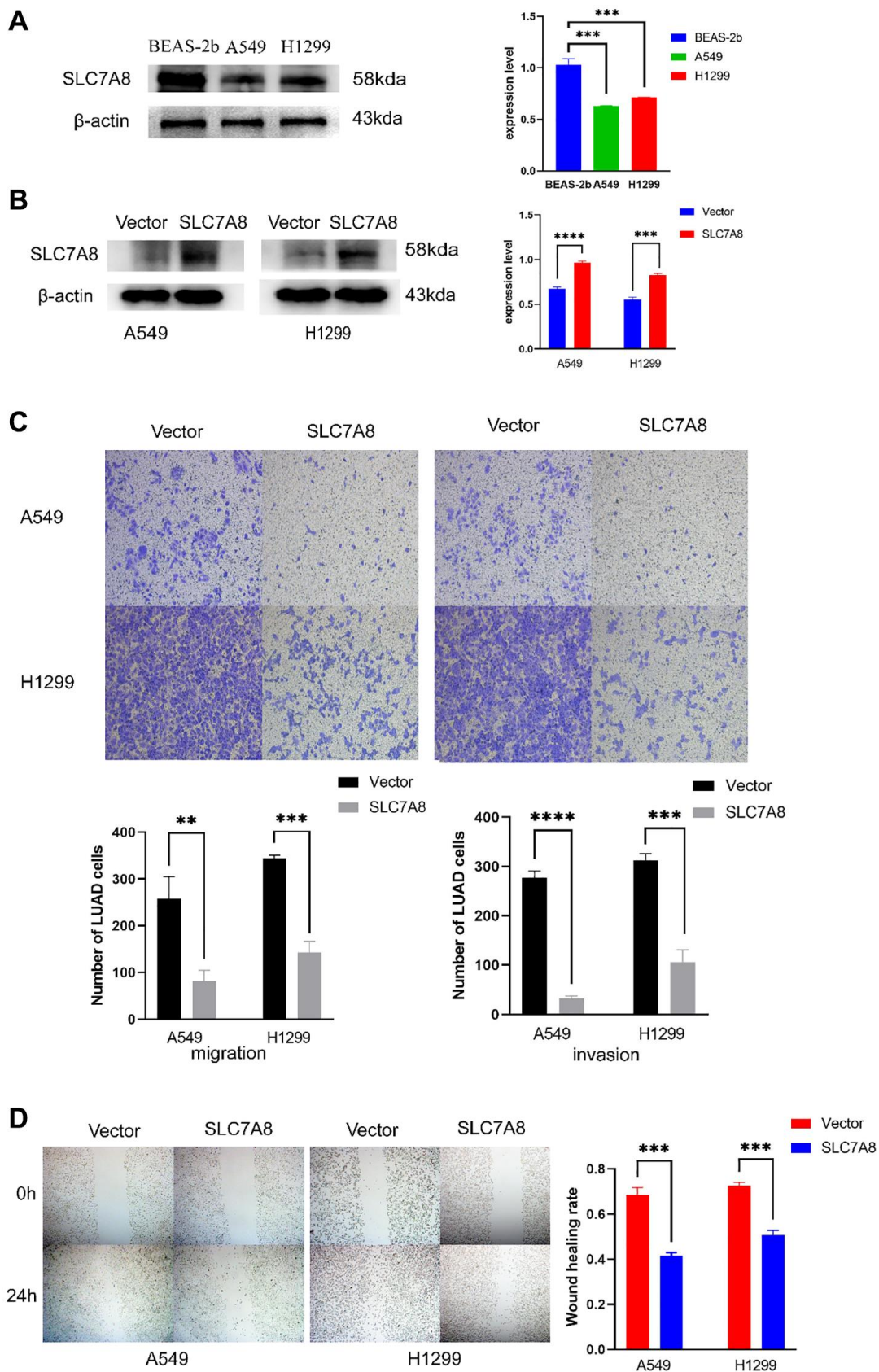


Figure 5. Overexpression of *SLC7A8* suppresses the migration and invasion of LUAD. (A) The expression level of *SLC7A8* in BEAS-2B, A549, and H1299 cells. (B) The protein expression levels were determined by Western blotting. (C) The migration and invasion were assessed using Transwell assays. (D) The migration ability was determined using wound healing assays as well.

Table 2. GO/KEGG analysis of *SLC7A8*.

Type	ID	Description	P-value
BP	GO:0018958	phenol-containing compound metabolic process	6.1974E-06
BP	GO:0030038	contractile actin filament bundle assembly	1.73008E-05
BP	GO:0043149	stress fiber assembly	1.73008E-05
BP	GO:0016999	antibiotic metabolic process	3.44352E-05
BP	GO:0006067	ethanol metabolic process	4.15677E-05
BP	GO:0017000	antibiotic biosynthetic process	4.15677E-05
BP	GO:0031638	zymogen activation	4.78141E-05
BP	GO:0006687	glycosphingolipid metabolic process	5.08109E-05
BP	GO:0006664	glycolipid metabolic process	5.9784E-05
BP	GO:1903509	liposaccharide metabolic process	6.57364E-05
BP	GO:0031032	actomyosin structure organization	9.37131E-05
BP	GO:0006643	membrane lipid metabolic process	0.000154598
BP	GO:0050665	hydrogen peroxide biosynthetic process	0.000160988
BP	GO:0072073	kidney epithelium development	0.00019478
BP	GO:0045056	transcytosis	0.000216961
BP	GO:0001655	urogenital system development	0.000220889
BP	GO:0006665	sphingolipid metabolic process	0.000222584
BP	GO:0072001	renal system development	0.000256287
BP	GO:0061337	cardiac conduction	0.000301821
BP	GO:0051492	regulation of stress fiber assembly	0.000393813
BP	GO:0032355	response to estradiol	0.000438313
BP	GO:0006068	ethanol catabolic process	0.000447416
BP	GO:0072520	seminiferous tubule development	0.000447416
BP	GO:0042403	thyroid hormone metabolic process	0.000475202
BP	GO:0051017	actin filament bundle assembly	0.000487038
BP	GO:0030324	lung development	0.000518227
BP	GO:0071560	cellular response to transforming growth factor beta stimulus	0.000542241
BP	GO:0042445	hormone metabolic process	0.000618613
BP	GO:0061572	actin filament bundle organization	0.000630999
BP	GO:0031670	cellular response to nutrient	0.000650715
BP	GO:0051145	smooth muscle cell differentiation	0.000650715
BP	GO:1901616	organic hydroxy compound catabolic process	0.000650715
BP	GO:0030323	respiratory tube development	0.000659255
BP	GO:0007015	actin filament organization	0.000692946
BP	GO:0071559	response to transforming growth factor beta	0.000724183
BP	GO:0051056	regulation of small GTPase mediated signal transduction	0.000749109
BP	GO:0060541	respiratory system development	0.000789527
BP	GO:0006631	fatty acid metabolic process	0.000820985
BP	GO:0021692	cerebellar Purkinje cell layer morphogenesis	0.000858959
BP	GO:0097202	activation of cysteine-type endopeptidase activity	0.000858959
BP	GO:0043268	positive regulation of potassium ion transport	0.000865894
CC	GO:0042599	lamellar body	0.000150683
CC	GO:0062023	collagen-containing extracellular matrix	0.000312972
KEGG	hsa00280	Valine, leucine and isoleucine degradation	4.78595E-06
KEGG	hsa00380	Tryptophan metabolism	1.1307E-05
KEGG	hsa00340	Histidine metabolism	8.15346E-05

KEGG	hsa05224	Breast cancer	0.000186964
KEGG	hsa00410	beta-Alanine metabolism	0.000512328
KEGG	hsa00071	Fatty acid degradation	0.000757955
KEGG	hsa00600	Sphingolipid metabolism	0.001463422
KEGG	hsa04142	Lysosome	0.00171453
KEGG	hsa05226	Gastric cancer	0.00214208
KEGG	hsa00620	Pyruvate metabolism	0.002161182
KEGG	hsa04115	p53 signaling pathway	0.003838081
KEGG	hsa04110	Cell cycle	0.004060117

Abbreviations: GO: Gene Ontology; KEGG: Kyoto Encyclopedia of Genes and Genomes.

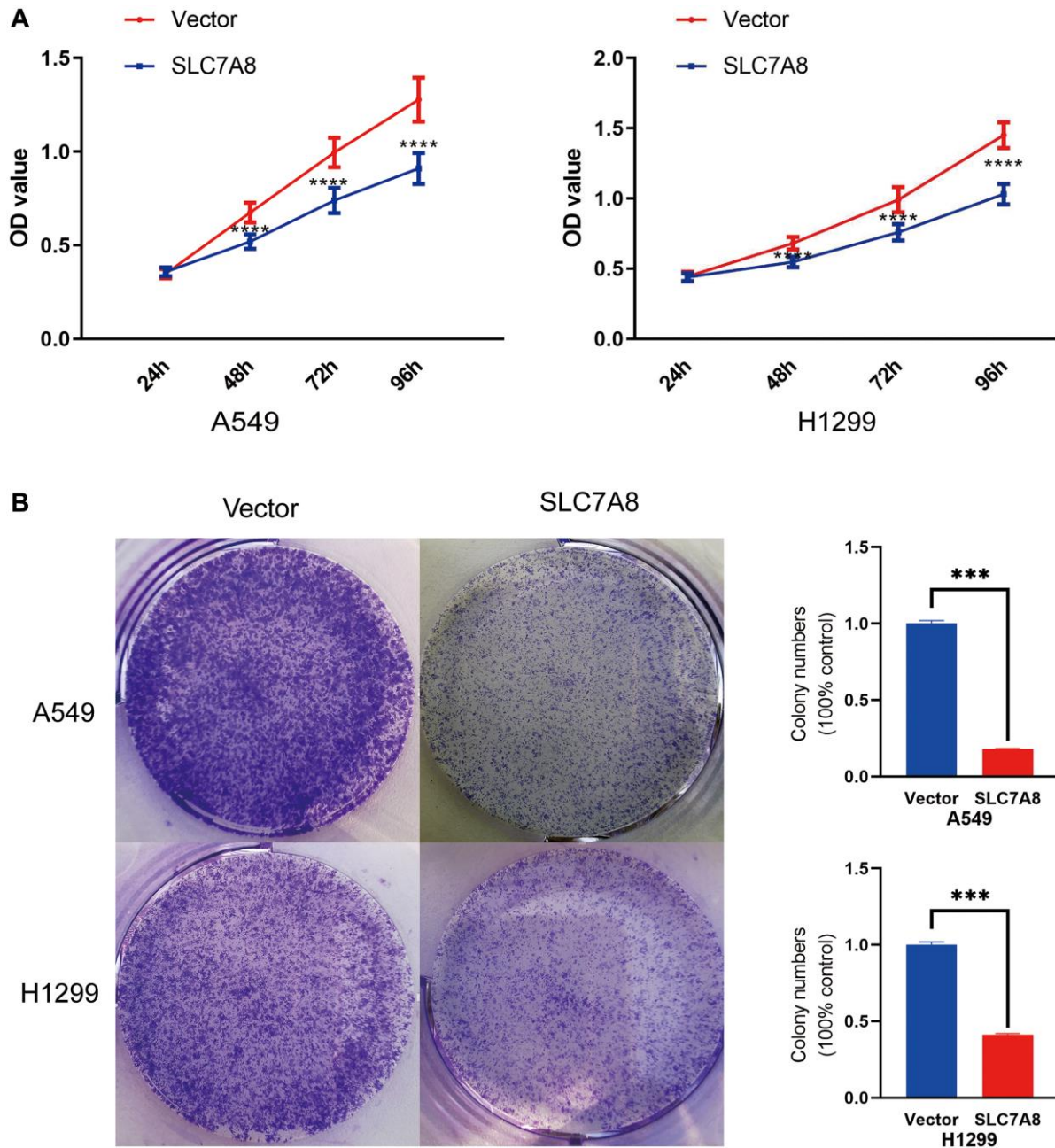


Figure 6. (A) Cell proliferation in the *SLC7A8*-overexpressing group was demonstrated using the CCK-8 assays. (B) Cell proliferation in the *SLC7A8*-overexpressing group was demonstrated using and colony forming assays. Abbreviation: CCK-8: Cell Counting Kit-8.

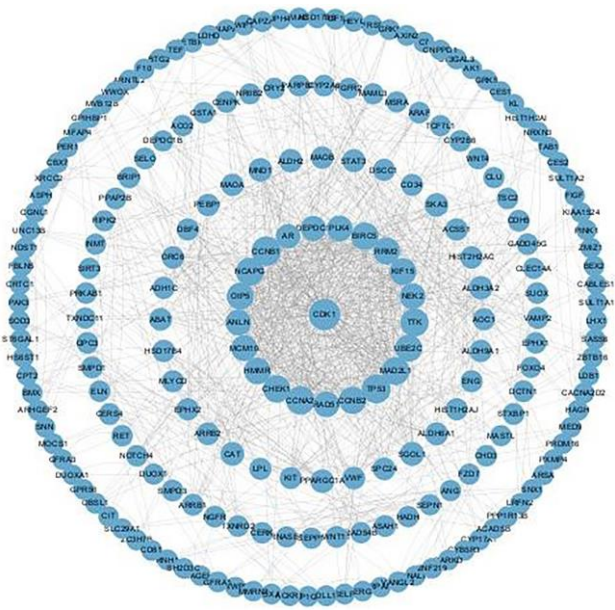


Figure 7. PPI network of genes strongly co-expressed with *SLC7A8*. Abbreviation: PPI: protein–protein interaction.

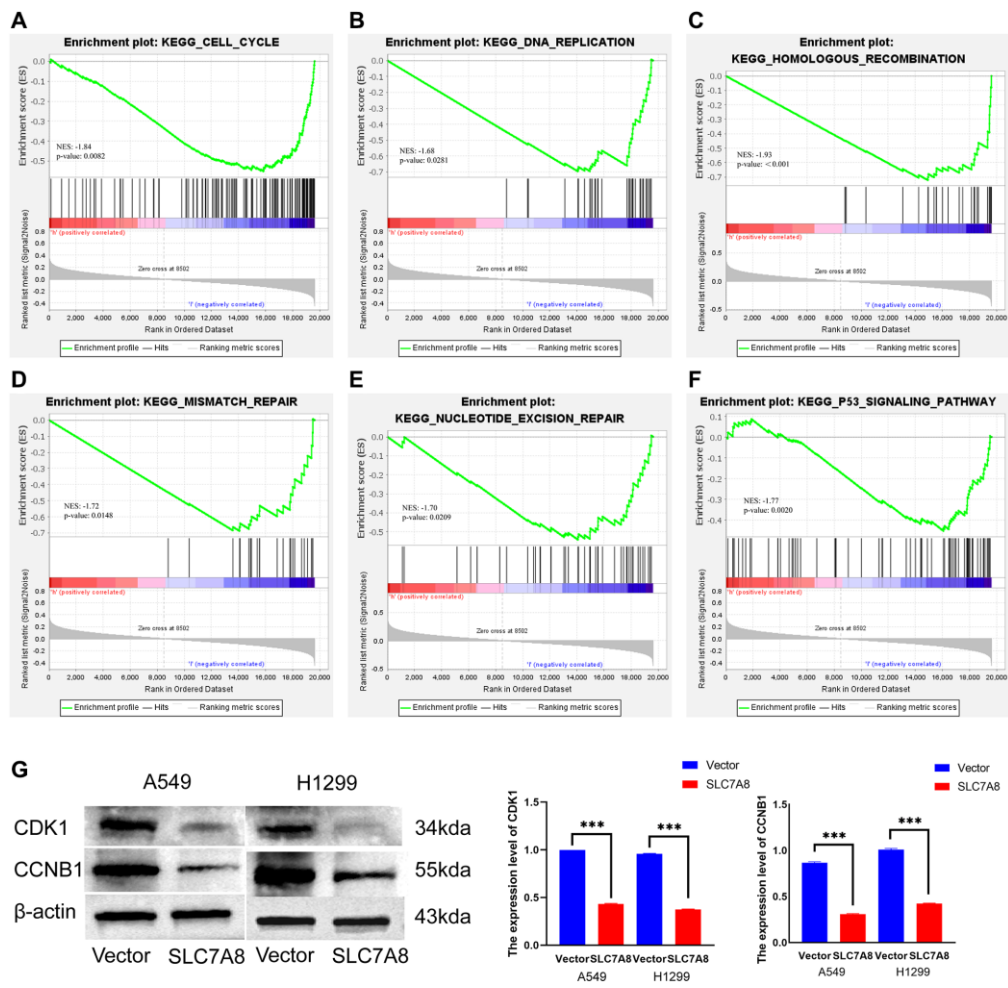


Figure 8. Mechanisms associated with *SLC7A8*. (A–F) Mechanisms associated with *SLC7A8* were explored using GSEA. (G) The expression levels of the cell cycle proteins CDK1 and CCNB1. Abbreviations: GSEA: Gene Set Enrichment Analysis; CDK1: cyclin-dependent kinase-1; CCNB1: cyclin B1.

experiments to validate these preliminary findings and found that the expression of cyclin-dependent kinase-1 (CDK1) and cyclin B1 (CCNB1), two important cell cycle proteins, was significantly attenuated in LUAD cells overexpressing *SLC7A8* (Figure 8G). These results suggest that overexpressing *SLC7A8* may potentially hinder the progression of LUAD by inhibiting the cell cycle pathway.

***SLC7A8* expression was correlated with infiltrated immune cells and immune factors in LUAD**

The expression level of *SLC7A8* was significantly correlated with the level of immune cell infiltration in LUAD, especially that of B cells, interstitial dendritic

cells, mast cells, CD56 bright cells, natural killer cells, plasmacytoid DCs, T follicular helper cells, T helper 2 cells, T helper17 cells (Figure 9). *SLC7A8* expression was also associated with some immune factors, such as CD5, CD34, CD36, CD37, CD79B, CDA, CDC7, CCL4, and CCL28 (Figure 10).

DISCUSSION

Although progress in the treatment and early screening of lung cancer have mitigated its incidence and mortality, it still accounts for a high percentage of cancer-related deaths [10]. Studies have identified some genes associated with cancer progression. *SLC7* genes were reported to be correlated with the prognosis of

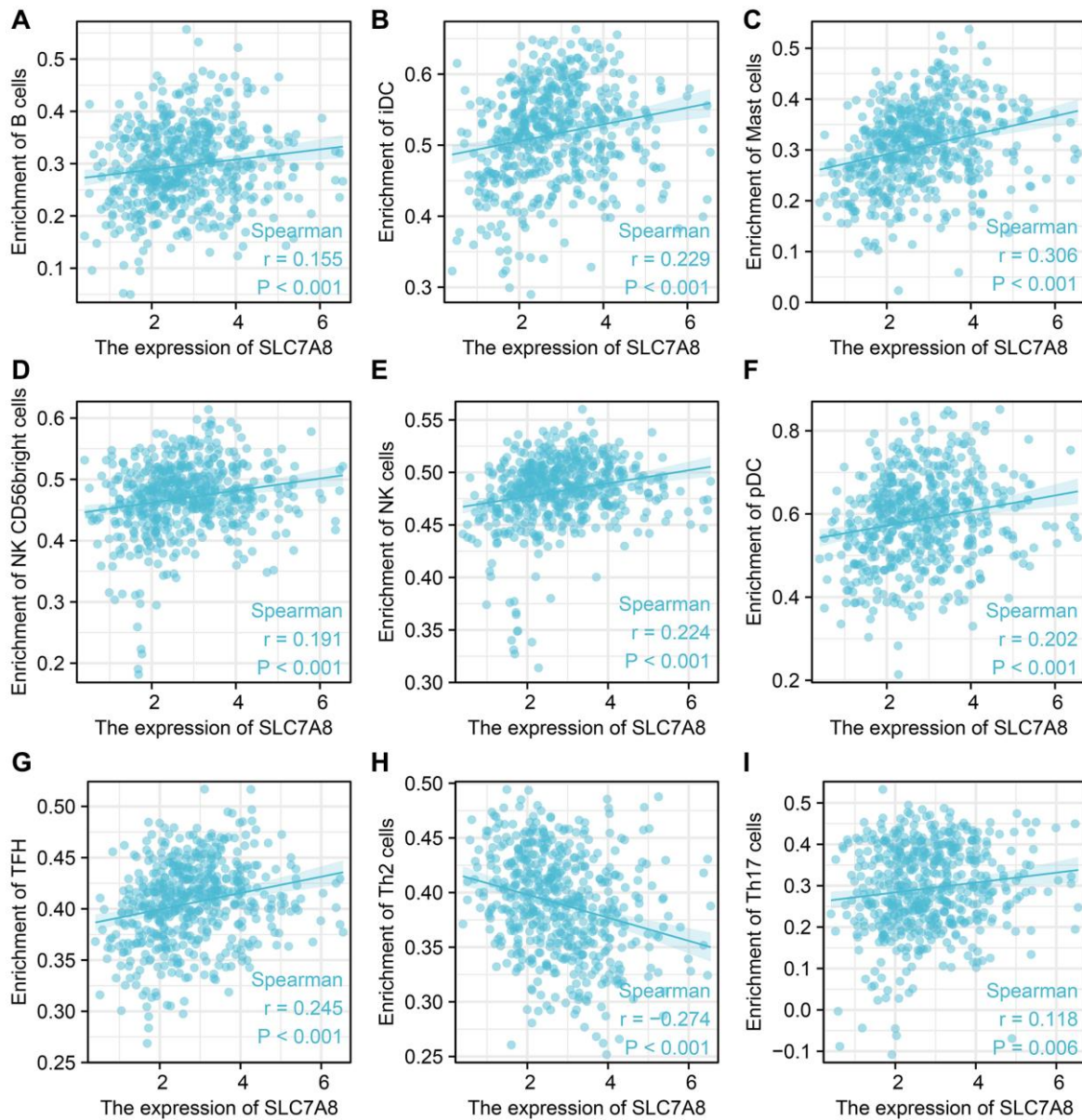


Figure 9. *SLC7A8* expression is correlated with immune infiltrated cells. (A) B cells. (B) iDC. (C) Mast cells. (D) NK CD56 bright cells. (E) NK cells. (F) pDC. (G) TFH. (H) Th2 cells. (I) Th17 cells.

lung cancer [11–14]. *SLC7A5* was overexpressed in LUAD and significantly correlated with the Ki-67 labeling index, which can increase metabolic activity and is associated with tumor cell growth [11]. *SLC7A8* was shown to be a good prognostic marker for breast cancer. When overexpressed, it behaved like a tumor suppressor, especially in low-growth ER-positive subtypes [6]. Jiang et al. found that *SLC7A2* increased drug sensitivity, immune infiltration, and survival in NSCLC [12]. The upregulation of *SLC7A7* increased the levels of arginine in tumor cells, thus promoting their migration and invasion [13]. Conversely, knockdown of *SLC7A9* inhibited the migration, invasion, and proliferation of esophageal squamous cell carcinoma cells, making it a suitable biomarker to predict lymph node metastasis of

this cancer [14]. Our studies showed that *SLC7A8* was lowly expressed in LUAD, whereas overexpression of *SLC7A8* was associated with higher OS, DSS, and PFI, making it a potential prognostic factor for LUAD.

The immune microenvironment intimately affects the progression of LUAD [15–17]. Cancer-related immune cells were shown to serve as biomarkers for the progression of NSCLC [18]. Genes from the *SLC7* family, such as *SLC7A11*, were shown to be associated with the immune microenvironment [19]. B cells, which are involved in humoral immunity, were shown to be an important component of the immune microenvironment of lung cancer. Moreover, differentiated plasma cells were shown to produce antibodies against tumor

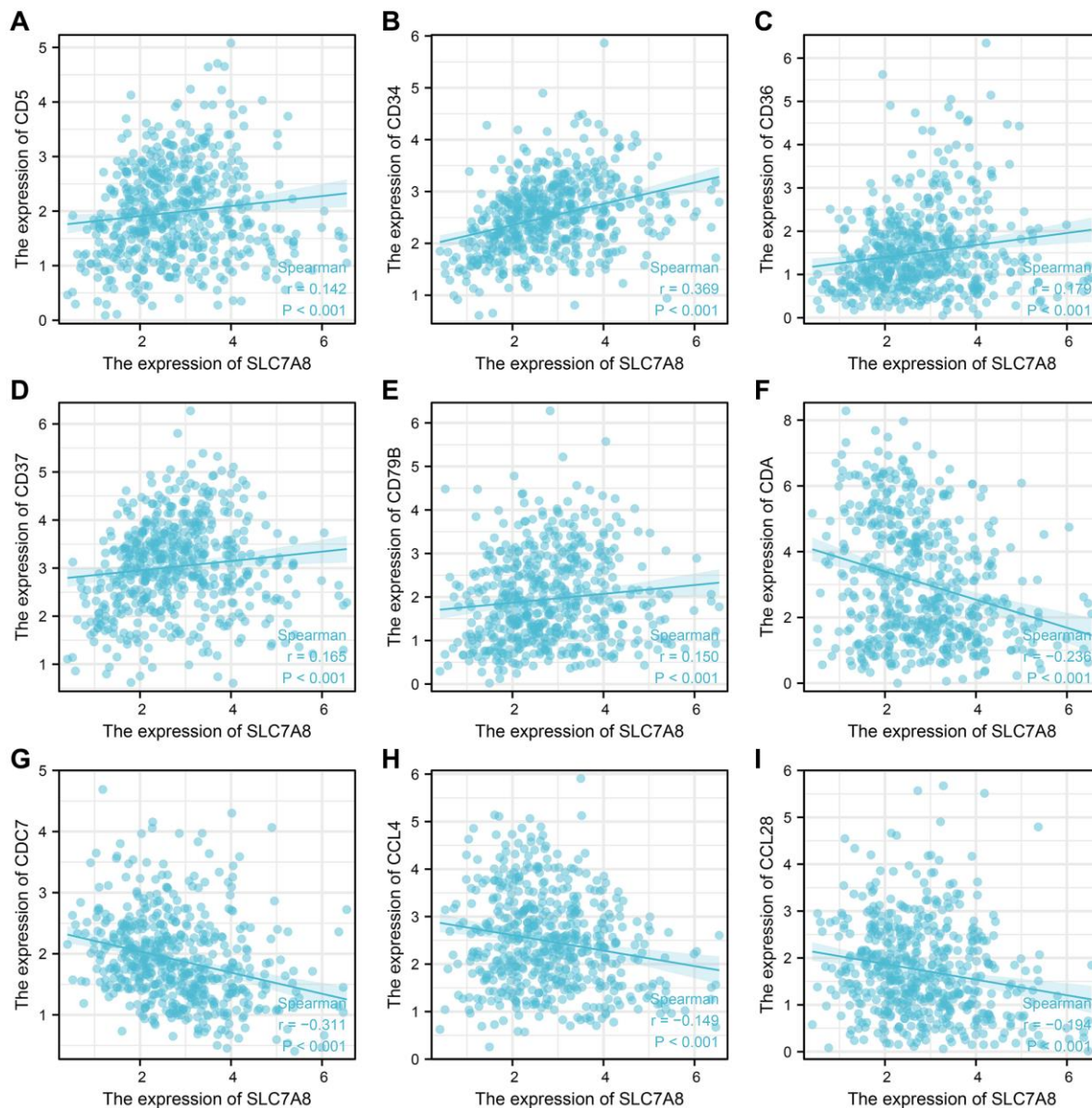


Figure 10. *SLC7A8* expression is correlated with immune factors. (A) CD5. (B) CD34. (C) CD36. (D) CD37. (E) CD79B. (F) CDA. (G) CDC7. (H) CCL4. (I) CCL28.

antigens, which contributed to the immune protection in lung cancer patients [20]. As an example of cell-mediated immunity, Th17 cells produced interleukin-22, which promoted the growth, migration, and invasion of tumor cells [21, 22]. Interleukin-22 also induced tumor cells to express CD155, which inhibits the function of NK cells and supports tumor cell metastasis [23]. In this study, we found that *SLC7A8* expression was associated with B cells, interstitial DCs, mast cells, CD56 bright cells, NK cells, plasmacytoid DCs, T follicular helper cells, Th2 cells, Th17 cells. Moreover, it was correlated with several immune factors, including CD5, CD34, CD36, CD37, CD79B, CDA, CDC7, CCL4, and CCL28. These results suggest that immune factors were significant in deciding the prognostic value of *SLC7A8* in LUAD. We believe that elucidating the relationship between *SLC7A8* and the immune micro-environment can lead to a breakthrough in the future treatment of LUAD.

Cancer is a disease characterized by dysregulated cell proliferation [24]. The knockdown of *CYP25I* effectively inhibited the migration, invasion, and proliferation of LUAD cells, while improving the OS of LUAD patients [25]. In this study, we found that the overexpression of *SLC7A8* also effectively inhibited the proliferation and migration of LUAD cells. Bioinformatic analysis showed that *SLC7A8* was closely associated with the cell cycle. Indeed, *SLC7A8* inhibited the expression of the cell cycle-related proteins CDK1 and CCNB1. Therefore, *SLC7A8* could check the progression of LUAD and improve its prognosis by influencing the proliferation and differentiation of LUAD cells.

This study has a couple of limitations. Firstly, although the relevant pathways were bioinformatically analyzed and experimentally verified, they were not validated through animal experiments, and we were unable to collect clinical samples for validation, which would have made the results more reliable. Secondly, we did not analyze extensive datasets, nor did we conduct multicenter cohort studies. Subsequent researchers may conduct multicenter studies based on this research.

This study demonstrated that the expression of *SLC7A8* was attenuated in LUAD tissues. *SLC7A8* can serve as a good prognostic marker for LUAD, and its overexpression inhibited the migration, invasion, and proliferation of LUAD cells.

MATERIALS AND METHODS

Data of LUAD patients

SLC7A8 expression data in LUAD tissues and normal lung tissues were downloaded from TCGA and Xena.

TCGA included 594 samples and Xena included 862 samples from the Genotype-Tissue Expression and TCGA databases. The clinical pathological and prognostic survival data of 522 LUAD patients were also downloaded from TCGA.

Identifying *SLC7A8* expression in LUAD

The expression levels of *SLC7A8* in normal lung tissues and LUAD tissues were determined by performing expression analysis on TPM data from TCGA and Xena. The expression of *SLC7A8* in human normal lung epithelial cell and LUAD were determined by Western blotting.

Evaluating the clinical value of *SLC7A8* in LUAD

After the LUAD patients were divided into groups according to their clinical pathological features, the expression levels of *SLC7A8* in LUAD tissues were determined based on TPM data from TCGA. The clinical diagnostic value of *SLC7A8* in LUAD was analyzed using ROC curves. Kaplan–Meier analysis and Cox regression were used to assess the prognostic value of *SLC7A8* in LUAD, and prognostic nomograms were constructed based on it.

Cell culture

The human lung epithelial cell line BEAS-2b was purchased from Abclonal (Abclonal, China). The LUAD cell lines A549 and H1299 were purchased from American Type Culture Collection (ATCC, China). BEAS-2b cells were cultured in DMEM (Gibco, Thermo Fisher Scientific, Inc., USA) with 10% FBS (Gibco, Thermo Fisher Scientific, USA) and 1% Penicillin-Streptomycin solution at 37°C with 5% CO₂. The LUAD cell lines were cultivated in Roswell Park Memorial Institute-1640 medium at 37°C with 5% CO₂.

Plasmid transfection

The *SLC7A8* expression plasmid and control vector were synthesized by RiboBio (China). A549 and H1299 cells were cultured in 6-well plates to about 80% confluence and transfected with 2 μg of plasmid using Lipofectamine[®]3000 (Thermo Fisher Scientific, USA) following standard protocols. After 6–8 h, the culture medium was replaced with a standard medium.

Western blotting

Total protein was extracted from A549, H1299, and BEAS-2b cells using RIPA buffer (Servicebio, China) and quantified using a BCA kit (Servicebio, China).

The proteins were resolved by SDS-PAGE (Servicebio, China), transferred to PVDF membranes (Millipore, USA), blocked with 5% milk powder, probed overnight at 4°C with anti-SLC7A8 (1:1000, Abclonal, China), anti-CCNB1 (1:1000, Abclonal, China), anti-CDK1 (1:1000, Abclonal, China), and anti-β-actin (1:1000, Proteintech, China), incubated at room temperature for 1 h with anti-Rabbit IgG (1:3000, Jackson, USA) and anti-Mouse IgG (1:3000, Jackson, USA) secondary antibodies, washed with Tris-buffered saline with Tween 20, and finally detected using an ECL kit (Beyotime, China).

Cell proliferation

The proliferation of A549 and H1299 cells was assessed using the CCK-8 and colony formation assays [26, 27]. For the CCK-8 assay, the transfected cells were seeded in 96-well plates and incubated with 10 μL of CCK-8 solution for 2 h. The absorbance was measured at 450 nm using a microplate reader at 24, 48, 72, and 96 h. For the colony formation assay, the transfected cells were seeded in 6-well plates, incubated for 14 days, and fixed for 1 h. The colonies were then photographed and counted.

Wound healing assay

Cells were seeded in 6-well plates and cultured for 12 h to reach 100% confluence. The “wound” was made by scratching the monolayer with a sterile 200-μL pipette tip. Photos were taken immediately (0 h) and 24 h later at 100× magnification. The healing rate (healing width at 0 h/healing width at 24 h) was calculated using ImageJ.

Transwell assay

The migration and invasion of A549 and H1299 cells were assessed using the Transwell assay [28]. To assess cell migration, the cells were cultured to the logarithmic growth phase, washed once each with phosphate-buffered saline and serum-free medium, suspended in serum-free medium at a concentration of 1×10^5 /mL, and seeded in the upper chamber of a 24-well Transwell chamber (Biosciences, USA). The lower chamber contained 600 μL of Roswell Park Memorial Institute-1640 medium containing 20% fetal bovine serum. After incubating for 24 h at 37°C, the lower chamber was fixed in 70% methanol for 1 h and stained with crystal violet. The cells in the low chamber were photographed and calculated. The protocol of the invasion assay was the same as that of the migration assay, except for the application of 100 μL of Matrigel to the upper surface of the membrane.

Roles, mechanisms, and PPI network of *SLC7A8*-related genes

Correlation analysis identified 679 genes coexpressed with *SLC7A8* in LUAD tissues. The coexpression was considered strong when the correlation value $r > 0.3$ or $r < -0.3$. The functions and mechanisms of the co-expressed genes were explored using Gene Ontology and Kyoto Encyclopedia of Genes and Genomes enrichment analysis, with $P < 0.05$ being the threshold for significance. The STRING database was used to construct a PPI network composed of the co-expressed genes, and Cytoscape was used for visualization. Based on the median value of *SLC7A8* expression, 535 LUAD cases from TCGA were sequenced and classified into two groups. GSEA was used to analyze the mechanisms of *SLC7A8* in LUAD progression.

Correlation between *SLC7A8* expression and immune infiltration in LUAD

LUAD tissues from TCGA were evaluated using single-sample GSEA, and the relationships between *SLC7A8* expression and immune cell infiltration were analyzed using Spearman’s correlation. Moreover, this method was applied to explore the relationships between *SLC7A8* expression and immune factors.

Statistical analysis

SLC7A8 expression in LUAD tissues was investigated using the *t*-test [29]. The diagnostic value of *SLC7A8* in LUAD was analyzed by computing the area under the ROC curves. The prognostic value of *SLC7A8* was ascertained using Cox regression and Kaplan–Meier survival analysis. The survival curves were constructed using the median grouping method, where 50% of patients were defined as having high expression of *SLC7A8* [30]. Correlation analysis was used to investigate the relationship between *SLC7A8* expression and immune cell infiltration in LUAD. $P < 0.05$ was considered to be significant.

Availability of data and materials

The datasets used during the current study are available from the corresponding authors upon reasonable request.

Abbreviations

SLC7A8: solute carrier family 7 member 8; LUAD: lung adenocarcinoma; ER: estrogen receptor; TCGA: The Cancer Genome Atlas; TPM: transcripts per million; ROC: receiver operating characteristic; CCK-8:

Cell Counting Kit-8; GSEA: Gene Set Enrichment Analysis; OS: overall survival; DSS: disease-specific survival; PFI: progression free interval; PPI: protein–protein interaction; NSCLC: non-small cell lung cancer.

AUTHOR CONTRIBUTIONS

Conception and design were done by Jiu-Ling Chen and Feng Zhao. Data acquisition and analysis was done by Fang-Ming Wang. Fang-Ming Wang, Li-Qiang Xu, and Zhong-Chao Zhang drafted the manuscript. Jiu-Ling Chen, Li-Qiang Xu, Qiang Guo, Zhi-Peng Du, Yue Lei, Chuang-Yan Wu, and Feng Zhao, revised the manuscript. The experiments were done by Zhi-Peng Du and Zhong-Chao Zhang, who contributed equally to this work. All authors have read and agreed to the final version of the manuscript.

ACKNOWLEDGMENTS

We acknowledge the participants and clinicians who contributed data to this study.

CONFLICTS OF INTEREST

The authors declare no conflicts of interest related to this study.

ETHICAL STATEMENT

All clinical information and data were obtained from public databases or purchased from commercial sources, and therefore, the ethical approval is not required for this study. All procedures performed in this study were in accordance with relevant research regulations.

FUNDING

This work was supported by the National Natural Science Foundation of China (No. 82100299).

REFERENCES

1. Sung H, Ferlay J, Siegel RL, Laversanne M, Soerjomataram I, Jemal A, Bray F. Global Cancer Statistics 2020: GLOBOCAN Estimates of Incidence and Mortality Worldwide for 36 Cancers in 185 Countries. *CA Cancer J Clin.* 2021; 71:209–49. <https://doi.org/10.3322/caac.21660> PMID:33538338
2. Chen Z, Fillmore CM, Hammerman PS, Kim CF, Wong KK. Non-small-cell lung cancers: a heterogeneous set of diseases. *Nat Rev Cancer.* 2014; 14:535–46. <https://doi.org/10.1038/nrc3775> PMID:25056707
3. Zhang L, Zhang Y, Wang C, Yang Y, Ni Y, Wang Z, Song T, Yao M, Liu Z, Chao N, Yang Y, Shao J, Li Z, et al. Integrated single-cell RNA sequencing analysis reveals distinct cellular and transcriptional modules associated with survival in lung cancer. *Signal Transduct Target Ther.* 2022; 7:9. <https://doi.org/10.1038/s41392-021-00824-9> PMID:35027529
4. He L, Chen J, Xu F, Li J, Li J. Prognostic Implication of a Metabolism-Associated Gene Signature in Lung Adenocarcinoma. *Mol Ther Oncolytics.* 2020; 19:265–77. <https://doi.org/10.1016/j.omto.2020.09.011> PMID:33209981
5. Breitenecker K, Homolya M, Luca AC, Lang V, Trenk C, Petroczi G, Mohrherr J, Horvath J, Moritsch S, Haas L, Kurnaeva M, Eferl R, Stoiber D, et al. Down-regulation of A20 promotes immune escape of lung adenocarcinomas. *Sci Transl Med.* 2021; 13:eabc3911. <https://doi.org/10.1126/scitranslmed.abc3911> PMID:34233950
6. El Ansari R, Alfarsi L, Craze ML, Masisi BK, Ellis IO, Rakha EA, Green AR. The solute carrier SLC7A8 is a marker of favourable prognosis in ER-positive low proliferative invasive breast cancer. *Breast Cancer Res Treat.* 2020; 181:1–12. <https://doi.org/10.1007/s10549-020-05586-6> PMID:32200487
7. Luo X, Yin P, Reierstad S, Ishikawa H, Lin Z, Pavone ME, Zhao H, Marsh EE, Bulun SE. Progesterone and mifepristone regulate L-type amino acid transporter 2 and 4F2 heavy chain expression in uterine leiomyoma cells. *J Clin Endocrinol Metab.* 2009; 94:4533–9. <https://doi.org/10.1210/jc.2009-1286> PMID:19808856
8. Min Q, Wang Y, Wu Q, Li X, Teng H, Fan J, Cao Y, Fan P, Zhan Q. Genomic and epigenomic evolution of acquired resistance to combination therapy in esophageal squamous cell carcinoma. *JCI Insight.* 2021; 6:e150203. <https://doi.org/10.1172/jci.insight.150203> PMID:34494553
9. Asada K, Kobayashi K, Joutard S, Tubaki M, Takahashi S, Takasawa K, Komatsu M, Kaneko S, Sese J, Hamamoto R. Uncovering Prognosis-Related Genes and Pathways by Multi-Omics Analysis in Lung Cancer. *Biomolecules.* 2020; 10:524. <https://doi.org/10.3390/biom10040524> PMID:32235589
10. Siegel RL, Miller KD, Fuchs HE, Jemal A. Cancer Statistics, 2021. *CA Cancer J Clin.* 2021; 71:7–33. <https://doi.org/10.3322/caac.21654> PMID:33433946

11. Nakanishi K, Matsuo H, Kanai Y, Endou H, Hiroi S, Tominaga S, Mukai M, Ikeda E, Ozeki Y, Aida S, Kawai T. LAT1 expression in normal lung and in atypical adenomatous hyperplasia and adenocarcinoma of the lung. *Virchows Arch*. 2006; 448:142–50. <https://doi.org/10.1007/s00428-005-0063-7> PMID:16175382
12. Jiang S, Zou J, Dong J, Shi H, Chen J, Li Y, Duan X, Li W. Lower SLC7A2 expression is associated with enhanced multidrug resistance, less immune infiltrates and worse prognosis of NSCLC. *Cell Commun Signal*. 2023; 21:9. <https://doi.org/10.1186/s12964-022-01023-x> PMID:36639771
13. Jahani M, Azadbakht M, Norooznezhad F, Mansouri K. l-arginine alters the effect of 5-fluorouracil on breast cancer cells in favor of apoptosis. *Biomed Pharmacother*. 2017; 88:114–23. <https://doi.org/10.1016/j.biopha.2017.01.047> PMID:28103504
14. Baba H, Kanda M, Sawaki K, Nakamura S, Ueda S, Shimizu D, Koike M, Kodera Y, Fujii T. SLC7A9 as a Potential Biomarker for Lymph Node Metastasis of Esophageal Squamous Cell Carcinoma. *Ann Surg Oncol*. 2022; 29:2699–709. <https://doi.org/10.1245/s10434-021-11001-1> PMID:34773193
15. Tang B, Xu W, Wang Y, Zhu J, Wang H, Tu J, Weng Q, Kong C, Yang Y, Qiu R, Zhao Z, Xu M, Ji J. Identification of critical ferroptosis regulators in lung adenocarcinoma that RRM2 facilitates tumor immune infiltration by inhibiting ferroptotic death. *Clin Immunol*. 2021; 232:108872. <https://doi.org/10.1016/j.jclim.2021.108872> PMID:34648954
16. Liu L, Xu S, Huang L, He J, Liu G, Ma S, Weng Y, Huang S. Systemic immune microenvironment and regulatory network analysis in patients with lung adenocarcinoma. *Transl Cancer Res*. 2021; 10:2859–72. <https://doi.org/10.21037/tcr-20-2275> PMID:35116596
17. Shen Y, Hou N, Han F, Chen B, Shi J, Sun X. Comprehensive Analysis of Tumor Immune Microenvironment and Prognosis of m6A-Related lncRNAs in Lung Adenocarcinoma. *Crit Rev Eukaryot Gene Expr*. 2022; 32:77–91. <https://doi.org/10.1615/CritRevEukaryotGeneExpr.20.22042417> PMID:35993946
18. Kiriu T, Yamamoto M, Nagano T, Hazama D, Sekiya R, Katsurada M, Tamura D, Tachihara M, Kobayashi K, Nishimura Y. The time-series behavior of neutrophil-to-lymphocyte ratio is useful as a predictive marker in non-small cell lung cancer. *PLoS One*. 2018; 13:e0193018. <https://doi.org/10.1371/journal.pone.0193018> PMID:29447258
19. He J, Ding H, Li H, Pan Z, Chen Q. Intra-Tumoral Expression of SLC7A11 Is Associated with Immune Microenvironment, Drug Resistance, and Prognosis in Cancers: A Pan-Cancer Analysis. *Front Genet*. 2021; 12:770857. <https://doi.org/10.3389/fgene.2021.770857> PMID:34938318
20. Germain C, Gnjatich S, Tamzalit F, Knockaert S, Remark R, Goc J, Lepelley A, Becht E, Katsahian S, Bizouard G, Validire P, Damotte D, Alifano M, et al. Presence of B cells in tertiary lymphoid structures is associated with a protective immunity in patients with lung cancer. *Am J Respir Crit Care Med*. 2014; 189:832–44. <https://doi.org/10.1164/rccm.201309-1611OC> PMID:24484236
21. Kryczek I, Lin Y, Nagarsheth N, Peng D, Zhao L, Zhao E, Vatan L, Szeliga W, Dou Y, Owens S, Zgodzinski W, Majewski M, Wallner G, et al. IL-22(+)CD4(+) T cells promote colorectal cancer stemness via STAT3 transcription factor activation and induction of the methyltransferase DOT1L. *Immunity*. 2014; 40:772–84. <https://doi.org/10.1016/j.immuni.2014.03.010> PMID:24816405
22. Kobold S, Völk S, Clauditz T, Küpper NJ, Minner S, Tufman A, Düwell P, Lindner M, Koch I, Heidegger S, Rothenfuer S, Schnurr M, Huber RM, et al. Interleukin-22 is frequently expressed in small- and large-cell lung cancer and promotes growth in chemotherapy-resistant cancer cells. *J Thorac Oncol*. 2013; 8:1032–42. <https://doi.org/10.1097/JTO.0b013e31829923c8> PMID:23774470
23. Briukhovetska D, Suarez-Gosalvez J, Voigt C, Markota A, Giannou AD, Schübel M, Jobst J, Zhang T, Dörr J, Märkl F, Majed L, Müller PJ, May P, et al. T cell-derived interleukin-22 drives the expression of CD155 by cancer cells to suppress NK cell function and promote metastasis. *Immunity*. 2023; 56:143–61.e11. <https://doi.org/10.1016/j.immuni.2022.12.010> PMID:36630913
24. Evan GI, Vousden KH. Proliferation, cell cycle and apoptosis in cancer. *Nature*. 2001; 411:342–8. <https://doi.org/10.1038/35077213> PMID:11357141
25. Guo H, Zeng B, Wang L, Ge C, Zuo X, Li Y, Ding W, Deng L, Zhang J, Qian X, Song X, Zhang P. Knockdown CYP25I1 inhibits lung cancer cells proliferation and migration. *Cancer Biomark*. 2021; 32:531–9.

- <https://doi.org/10.3233/CBM-210189>
PMID:34275895
26. Liu Y, Liang L, Ji L, Zhang F, Chen D, Duan S, Shen H, Liang Y, Chen Y. Potentiated lung adenocarcinoma (LUAD) cell growth, migration and invasion by lncRNA DARS-AS1 via miR-188-5p/ KLF12 axis. *Aging (Albany NY)*. 2021; 13:23376–92.
<https://doi.org/10.18632/aging.203632>
PMID:34644678
27. Huo X, Wang H, Huo B, Wang L, Yang K, Wang J, Wang L, Wang H. FTX contributes to cell proliferation and migration in lung adenocarcinoma via targeting miR-335-5p/NUCB2 axis. *Cancer Cell Int*. 2020; 20:89.
<https://doi.org/10.1186/s12935-020-1130-5>
PMID:32226311
28. Liang J, Li H, Han J, Jiang J, Wang J, Li Y, Feng Z, Zhao R, Sun Z, Lv B, Tian H. Mex3a interacts with LAMA2 to promote lung adenocarcinoma metastasis via PI3K/AKT pathway. *Cell Death Dis*. 2020; 11:614.
<https://doi.org/10.1038/s41419-020-02858-3>
PMID:32792503
29. Guo Q, Wu CY, Jiang N, Tong S, Wan JH, Xiao XY, Mei PY, Liu HS, Wang SH. Downregulation of T-cell cytotoxic marker IL18R1 promotes cancer proliferation and migration and is associated with dismal prognosis and immunity in lung squamous cell carcinoma. *Front Immunol*. 2022; 13:986447.
<https://doi.org/10.3389/fimmu.2022.986447>
PMID:36544782
30. Yousef GM, Scorilas A, Katsaros D, Fracchioli S, Iskander L, Borgono C, Rigault de la Longrais IA, Puopolo M, Massobrio M, Diamandis EP. Prognostic value of the human kallikrein gene 15 expression in ovarian cancer. *J Clin Oncol*. 2003; 21:3119–26.
<https://doi.org/10.1200/JCO.2003.09.111>
PMID:12915603